PROTEINS: Structure, Function, and Bioinformatics 55:177–186 (2004)

Trehalose–Protein Interaction in Aqueous Solution

Roberto D. Lins, Cristina S. Pereira,[†] and Philippe H. Hünenberger[*]
Laboratory of Physical Chemistry, ETH-Hönggerberg, Zürich, Switzerland

ABSTRACT **A variety of sugars are known to enhance the stability of biomaterials. Trehalose, a nonreducing disaccharide composed of two α, α(1 → 1)-linked D-glucopyranose units, appears to be one of the most effective protectants. Both in vivo and in vitro, trehalose protects biostructures such as proteins and membranes from damage due to dehydration, heat, or cold. However, despite the significant amount of experimental data on this disaccharide, no clear picture of the molecular mechanism responsible for its stabilizing properties has emerged yet. Three major hypotheses (water–trehalose hydrogen-bond replacement, coating by a trapped water layer, and mechanical inhibition of the conformational fluctuations) have been proposed to explain the stabilizing effect of trehalose on proteins. To investigate the nature of protein–trehalose–water interactions in solution at the molecular level, two molecular dynamics simulations of the protein lysozyme in solution at room temperature have been carried out, one in the presence (about 0.5 *M*) and one in the absence of trehalose. The results show that the trehalose molecules cluster and move toward the protein, but neither completely expel water from the protein surface nor form hydrogen bonds with the protein. Furthermore, the coating by trehalose does not significantly reduce the conformational fluctuations of the protein compared to the trehalose-free system. Based on these observations, a model is proposed for the interaction of trehalose molecules with a protein in moderately concentrated solutions, at room temperature and on the nanosecond timescale. Proteins 2004;55:177–186.**

Key words: anhydrobiosis; trehalose; lysozyme; protein stability; carbohydrates; molecular dynamics

INTRODUCTION

Trehalose is a naturally occurring, nonreducing disaccharide composed of two D-glucopyranose units in α, α(1 → 1) linkage, which possesses particularly interesting physicochemical and biological properties.[1–3] The phase diagram of this compound presents peculiar features.[4] Trehalose dihydrate first melts at 97°C. However, upon additional heating, the disaccharide recrystallizes at 130°C in an anhydrous form, that melts again at 203°C.[3] The difficulty to perform its hydrolysis in acidic solutions and the inability of α-glucosidase to cleave its glycosidic bond also make trehalose a highly stable disaccharide.[3,5] Finally, this compound is characterized by an unusually high degree of optical rotation.[3]

In nature, trehalose constitutes the main sugar present in the hemolymph of insects (about 80–90% of the overall sugar content) and can comprise up to 20% of all carbohydrates during specific stages of their development.[6] Trehalose is also present in large amounts (up to 20% of the dry mass) in certain desert plants[7] and some organisms, such as tardigrades,[8] the shrimp *Artemia salina*,[9,10] yeasts, algae, and fungi,[5,6] capable of surviving almost complete dehydration at elevated temperatures, a phenomenon known as anhydrobiosis.[11,12] Under these extreme conditions, the biological function of the organism is interrupted. However, trehalose is able to stabilize biological structures in the dehydrated form, and to restore them intact and functional as soon as the hydration and temperature conditions return to the normal. The protective effect of trehalose manifests itself mainly at two levels, namely, the stabilization of membranes and lipid assemblies at very low hydration,[13–15] and the stabilization of biological macromolecules (e.g., proteins) in the folded state under conditions that would normally promote their denaturation.[16–18] Additionally, in some freeze-tolerant organisms, trehalose plays a similar role as a cryoprotectant.[18,19] Because trehalose appears to act on widely different classes of biostructures, the protective mechanism of this disaccharide against the stress of dehydration, heating, or freezing has been described as a nonspecific process.[20]

These very particular properties of trehalose make it a candidate for numerous practical applications, including (1) the preservation of delicate biological structures (proteins, living cells) in a dehydrated form at ambient temperature; (2) the protection of biological samples during experiments in vacuum; (3) the use of trehalose-based glasses for the crystallogenesis of proteins and membrane-based systems; (4) the coating of dried food to slow down the degradation and escape of flavors; and (5) the use as a cryoprotectant. Stabilization (and even activation) of thermolabile enzymes at elevated temperatures in trehalose solution has already found applications in biotechnology.[21]

Grant sponsor: Swiss National Foundation; Grant number: 21–63 408. Grant sponsor: Capes Agency (CSP).

[†]On leave: Departamento de Quimica, Universidade Federal de São Carlos, Brazil.

*Correspondence to: Philippe H. Hünenberger, Laboratory of Physical Chemistry, ETH-Hönggerberg, HCI G233, CH-8093 Zürich, Switzerland. E-mail: phil@igc.ethz.ch

Received 18 June 2003; Accepted 3 September 2003

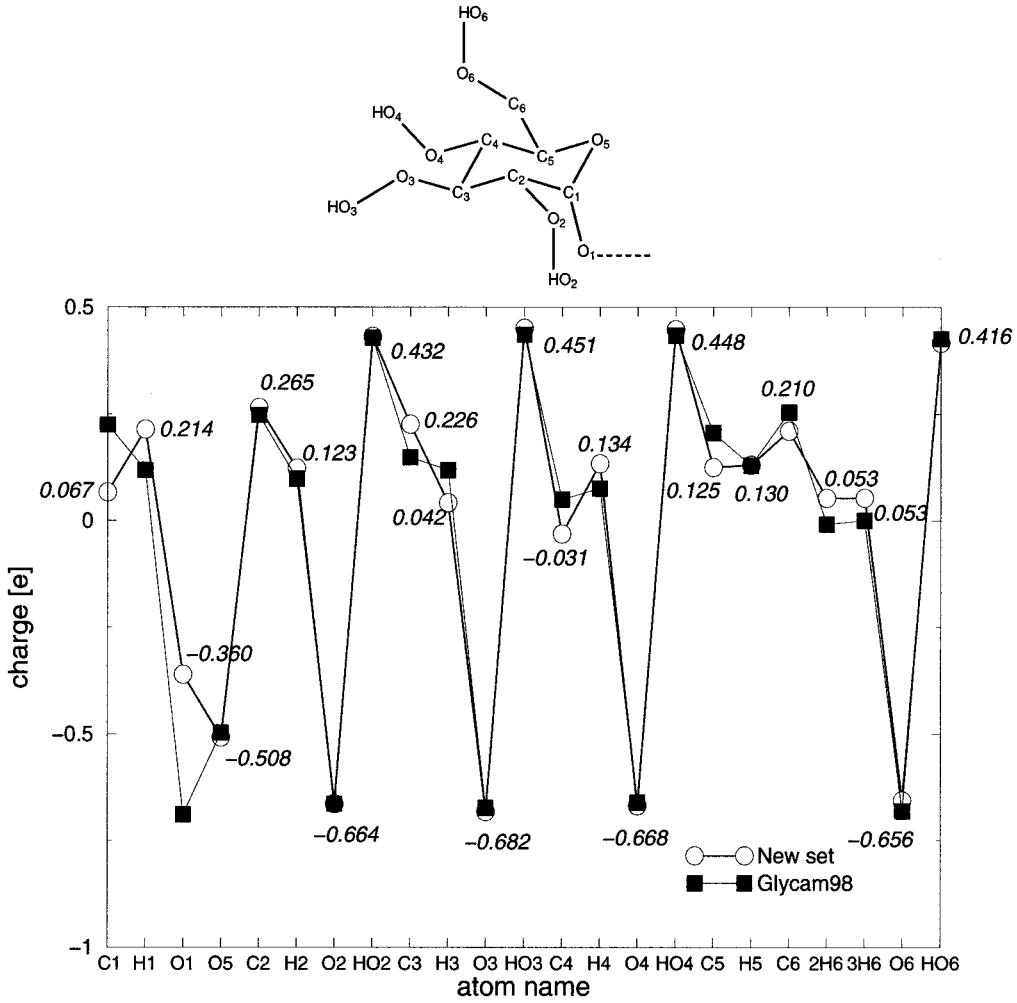

Fig. 1. Comparison between the atomic charge set derived in this study for the trehalose molecule and the Glycam98[33] charge set for the glucose molecule.

Trehalose has also made its way into a line of cosmetic products.[22]

Although the influence of trehalose on biomolecules has been extensively investigated, the detailed mechanism (at the molecular level) responsible for the protecting ability of this disaccharide remains unknown. Currently available experimental techniques have often led to contradictory conclusions. Three main hypotheses have been put forward involving (1) the direct interaction between trehalose molecules and the protected biostructure through hydrogen bonds (water-replacement hypothesis)[23–26]; (2) the trapping of water molecules close to the biomolecular surface (water-layer hypothesis)[27]; and (3) the entrapment of a particular biomolecular conformation in a high-viscosity trehalose glass (mechanical-entrapment hypothesis).[28,29]

The aim of this study is to better understand the role of trehalose in enhancing the stability of proteins. To this purpose, atomistic molecular dynamics (MD) simulations of aqueous hen egg-white lysozyme in the presence or absence of trehalose have been performed. The results of these simulations are compared to the three above-mentioned hypotheses for the stabilizing effect of this additive (and their supporting experimental evidences). Finally, a model for trehalose–protein interaction in aqueous solution is presented.

METHODS

Molecular Systems

The crystal structure of hen egg-white lysozyme with Protein Data Bank (PDB) entry code 194L, solved at 1.40 Å resolution,[30] was used as a starting point for all simulations. Two systems were considered: a protein–water system and a protein–trehalose–water system with a trehalose concentration of about 0.5 *M*. In both cases, simulations were performed under periodic boundary conditions based on a cubic box of initial edge lengths 7.2 nm. Trehalose molecules, when included, were uniformly distributed throughout the box, keeping a distance of at least 0.5 nm from the protein surface and from each other. The system was then solvated by filling the box with extended simple-point-charge (SPC/E) water molecules,[31] imposing a minimum distance of 0.28 nm between water molecules and any solute atom, and preserving the coordinates of the

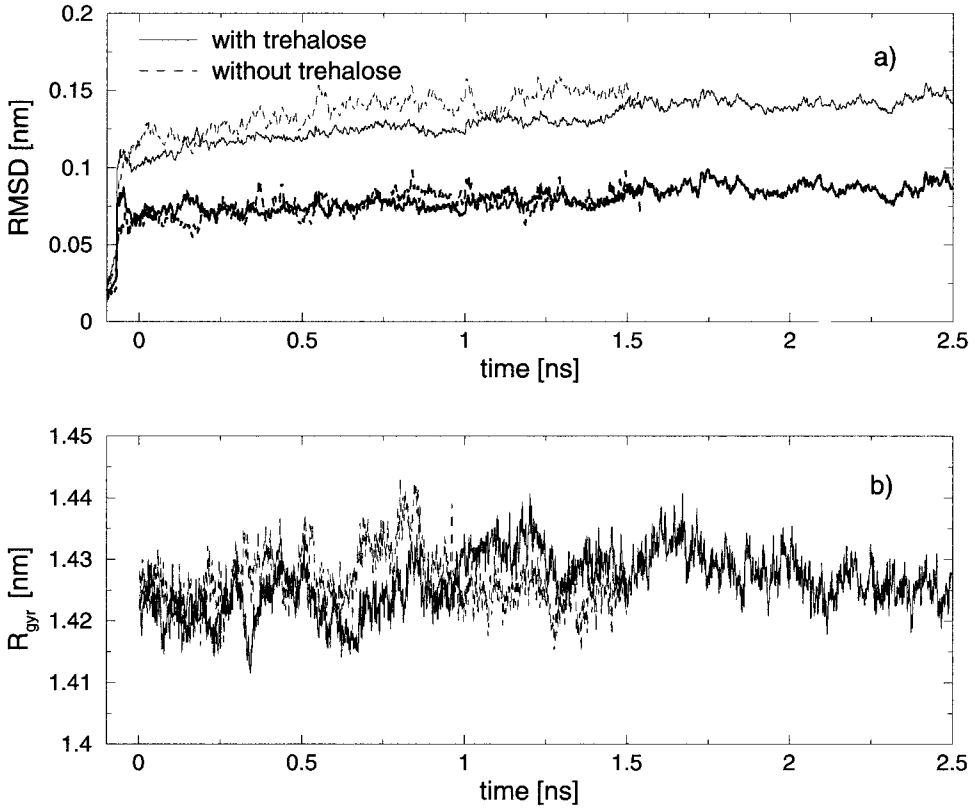

Fig. 2. (**a**) Root-mean-square atomic positional deviation (RMSD) from the crystallographic structure and (**b**) radius of gyration (R_{gyr}) as a function of time for the simulations in the presence or absence of trehalose. The RMSD is calculated either for all protein atoms (thin lines) or for C_α carbon atoms only (thick lines).

139 crystallographic water molecules. Finally the 8 water molecules with the highest electrostatic potential at the oxygen site, and a minimum distance of 1.0 nm from any protein atom, were successively replaced by chloride ions in order to neutralize the system. This procedure resulted in a system of 1 protein molecule, 106 trehalose molecules, 8 chloride ions, and 9319 water molecules (35,695 atoms) for the system with trehalose, and 1 protein molecule, 8 chloride ions, and 11,663 water molecules (36,960 atoms) for the system without trehalose.

Molecular Dynamics Simulations

All simulations were performed using the AMBER96 force field[32] in conjuction with a modified version (trehalose-optimized charge set; see below) of the Glycam98 force field[33] implemented in the parallel NWChem4.1 program[34] on 28 nodes of an IBM SP2 computer. The systems were equilibrated in a stepwise fashion. First, the solvent was relaxed using 200 steps of steepest descent energy minimization, keeping the protein, trehalose (when present), and counterions fixed. This was followed by an additional 200 steps of minimization without solute constraints. Solvent equilibration keeping protein, trehalose (when present), and chloride ions fixed was continued by performing 20 ps MD simulation at 298 K. Successive 5 ps equilibration periods of the solute (solvent fixed) were then performed at 50, 100, 150, 200, 250, and 298 K, with velocity reassignments every 0.5 ps. Finally, the whole system (solute and solvent) was equilibrated for 50 ps at 298 K. Following the total 100 ps equilibration time, production MD runs were carried out in the isothermal–isobaric ensemble for 1.5 and 2.5 ns, respectively, for the systems in the absence and in the presence of trehalose. The temperature was maintained at 298 K by weak coupling the solute and solvent separately to a heat bath,[35] with a relaxation time of 0.1 ps. The pressure was kept at $1.025 \cdot 10^5$ Pa using weak coupling to a pressure bath[35] via isotropic coordinate scaling with a relaxation time of 0.4 ps. Long-range electrostatic interactions were handled using the smooth particle mesh Ewald (SPME) method.[36] A cutoff 1.0 nm was used for the short-range nonbonded interactions (van der Waals and real-space electrostatic contribution). The SHAKE[37] algorithm was applied to constrain all bonds involving a hydrogen atom, and a 2-fs timestep was used to integrate the equations of motion based on the leapfrog algorithm.[38] Trajectory frames were recorded every 0.2 ps for analysis.

Charge Model

The present simulations were carried out using the Glycam98 force field[33] to describe the trehalose molecule, except for the charges, which were reoptimized for the specific case of this disaccharide. Charge sets in carbohydrate force fields have often been derived based either on

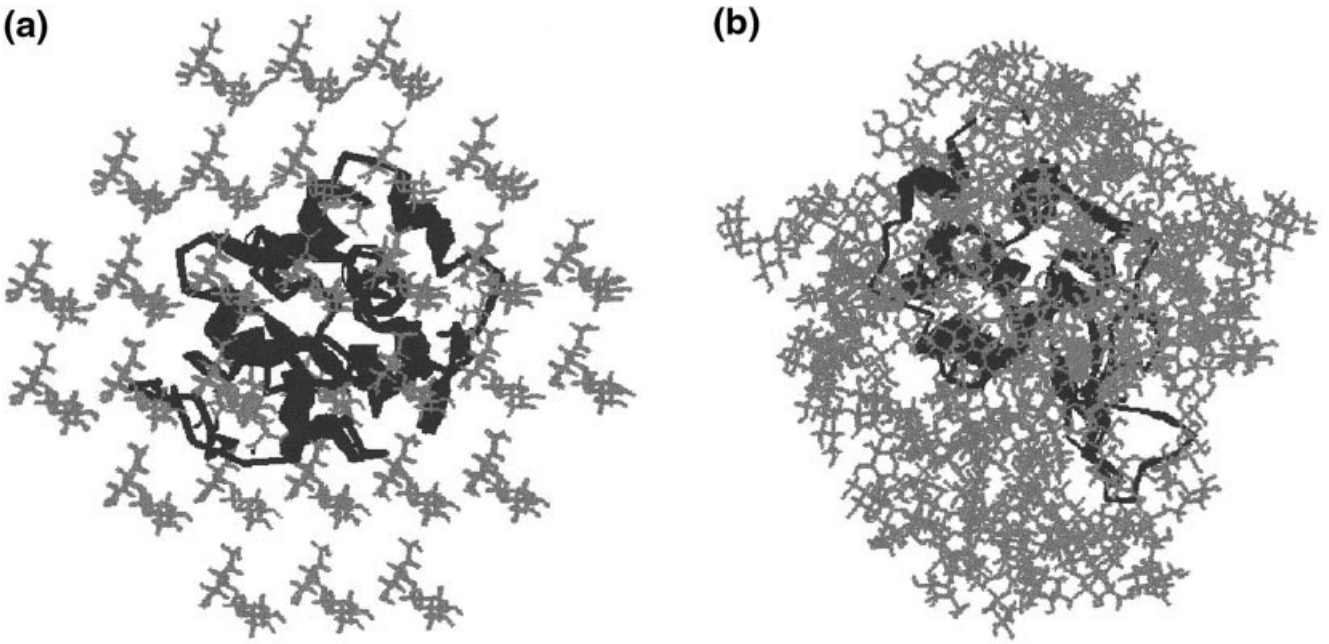

Fig. 3. (**a**) Initial and (**b**) final configurations of the protein–trehalose–water system. Water molecules have been removed for clarity.

small fragments[39,40] or on the glucose molecule.[33,41] However, trehalose (as well as residues in oligo- and polysaccharides) has one hydroxyl group functionalized into a glycosidic bond. Such a modification in the chemical environment of the group is expected to significantly alter its electrostatic properties. To remedy this problem, Hartree–Fock calculations on trehalose at the 6-31G* level, and a restrained electrostatic potential (RESP) fit[42] based on the opimized geometry, were performed using the NWChem4.1 program[34] to compute a first set of partial charges. A 1 ns MD simulation of trehalose in a box of 869 SPC/E water molecules[31] at 298 K was then carried out based on this initial charge set. The charge derivation procedure was then repeated for the two energy–minimized average structures corresponding to the 0–0.5 ns and 0.5–1.0 ns intervals of this new simulation, and the two charge sets were averaged to produce a final trehalose charge set. Values of 0.005 *a.u.* for the harmonic and 0.001 *a.u.* for the hyperbolic restraints, respectively, were used for all RESP fittings.

A second 1 ns MD simulation was performed based on this final charge set, starting from an initially distorted structure ($\Phi = 240°$ and $\Phi' = 300°$ with Φ and Φ' defined by atoms O5-C1-O1-C1′ and C1-O1-C1′-O5, respectively), which converged to the experimental structure within 100 ps. The corresponding average values of the glycosidic dihedral angles, $\Phi = \Phi' = 51 \pm 9°$ were found to be in good agreement with the values determined by NMR ($\Phi = \Phi' = 41 \pm 5°$) and optical rotary dispersion ($\Phi = \Phi' = 60°$).[43,44] This final charge set is compared to the corresponding set for the glucose molecule in Glycam98[33] in Figure 1. The two sets are very similar for the majority of the atoms. The most significant differences are confined, as expected, to the region of the glycosidic linkage. Charge derivation by means of RESP fitting[42] preserves the dipole moment of a molecule to its quantum-mechanical value, and should therefore lead to a realistic description of intermolecular interactions with identical as well as distinct molecular species during a simulation. The whole charge-derivation procedure was performed according to the AMBER96/Glycam98 force fields philosophy[32,33] in order to preserve force field compatibility.

RESULTS AND DISCUSSION

Deviation From the Initial Structure

After the initial equilibration period of 100 ps, no significant drifts were observed in the total potential energy of the system, and in the individual contributions to the potential and nonbonded solute–solute and solute–solvent interaction energies (data not shown). The root-mean-square atomic positional deviation (RMSD) from the crystallographic structure, for either all atoms or C_α atoms only, is displayed as a function of time in Figure 2(a). Convergence of the RMSD for the C_α atoms essentially occurred within the 0.1 ns equilibration time (to about 0.08 nm), and only a moderate drift was observed thereafter. The RMSD for all atoms also essentially converged within the equilibration time. However, the all-atom RMSD value for the simulation in the presence of trehalose is systematically lower by about 0.02 nm compared to the simulation without the disaccharide, while no such difference is observed for the C_α RMSD. The protein radius of gyration is displayed as a function of time in Figure 2(b). No significant drift was detected during the entire simulation, and both simulations led to very similar values for this quantity. The secondary structure, as probed using the DSSP program,[45] was equally-well maintained for both systems throughout the entire trajectories (data not shown). This finding is in good agreement with two recent crystallographic studies of lysozyme in the presence and

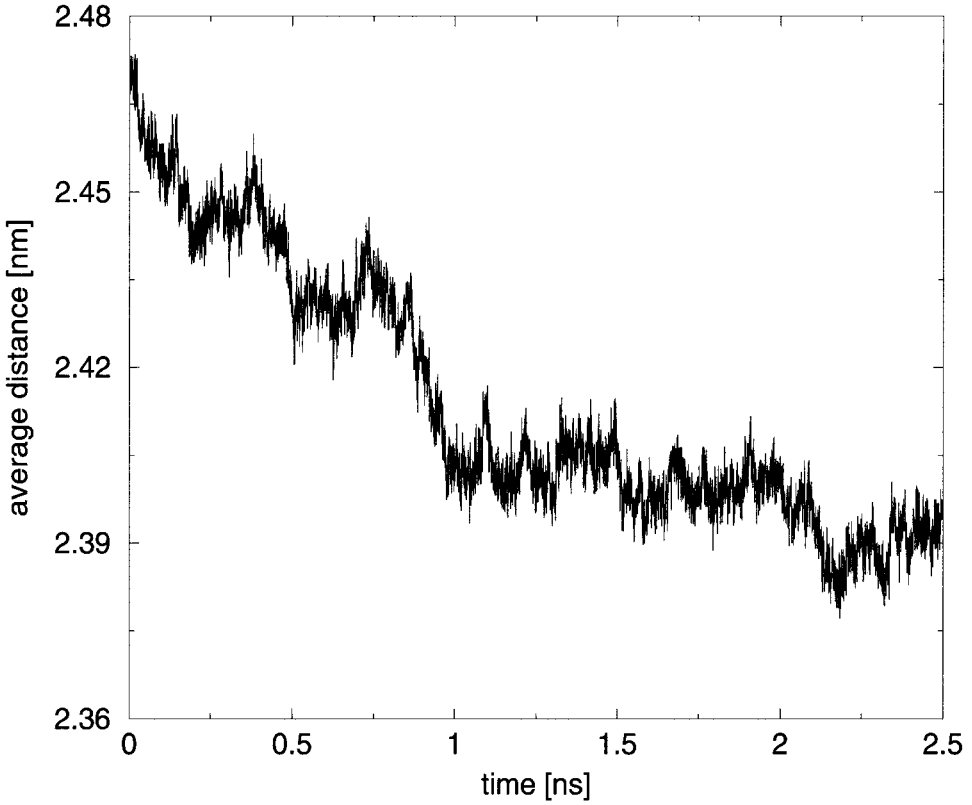

Fig. 4. Average distance between the trehalose oxygen atoms and the center of geometry of the protein as a function of time for the simulation including trehalose.

absence of trehalose. Although the atomic thermal factors were found to be slightly lower for the protein in the presence of the stabilizing additive, the protein structure remained essentially unaffected by the presence of trehalose.[46,47] The stability of the energies, RMSD, radius of gyration, and secondary structure content suggests that the protein has achieved structural and energetical equilibrium within the 0.1 ns equilibration time, with reasonably small deviations from the crystallographic structure.

Trehalose–Protein Interactions

The initial configuration of the protein–trehalose system was obtained by uniformly distributing the trehalose molecules within the computational box [Fig. 3(a)]. The average distance between the trehalose oxygen atoms and the center of geometry of the protein is displayed in Figure 4 as a function of time. This curve indicates that the trehalose molecules tend to cluster with each other and move toward the protein surface within the first nanosecond of the simulation. This new arrangement [Fig. 3(b)] appears to be essentially stable throughout the rest of the simulation (Fig. 4).

The radial distribution functions, $g(r)$, corresponding to the water and trehalose oxygens around the center of geometry of the protein are displayed in Figure 5 for the initial and equilibrated trehalose configurations, and for both the simulations including or excluding trehalose. The initial and equilibrated water distributions in the absence of trehalose [Fig. 5(a)] are, as expected, nearly indistinguishable. The two curves differ from the initial water distribution in the system with trehalose [Fig. 5(b)], but only because a number of water molecules in the approximate range 1.5–3.5 nm have been replaced by trehalose molecules. Comparing the initial and final distributions for the system containing trehalose [Fig. 5(b) and 5(c)], the following observations can be made: a shift of the trehalose distribution toward the protein surface (as anticipated from Fig. 3 and 4); a shift of the water distribution away from the protein (reduced density in the approximate range 1.5–2.4 nm, increased density in the approximate range 2.4–3.1 nm). However, the water density in the approximate range 0.0–1.5 nm is essentially unaffected, indicating that (on the nanosecond timescale) the most tightly bound water molecules are not displaced, and form a thin layer of about 125 water molecules [as estimated by the integral of $4\pi r^2 g(r)$ in this range] between the protein (exposed and reentrant) surface and the trehalose coating layer.

The time-evolution of the number of hydrogen bonds within the system containing trehalose is presented in Figure 6 and provides further insight into the ongoing process. The corresponding overall variations in the number of hydrogen bonds during the entire simulation are reported in Table I. Unexpectedly, although the trehalose molecules cluster around the protein surface, the number of direct protein–trehalose hydrogen bonds does not in-

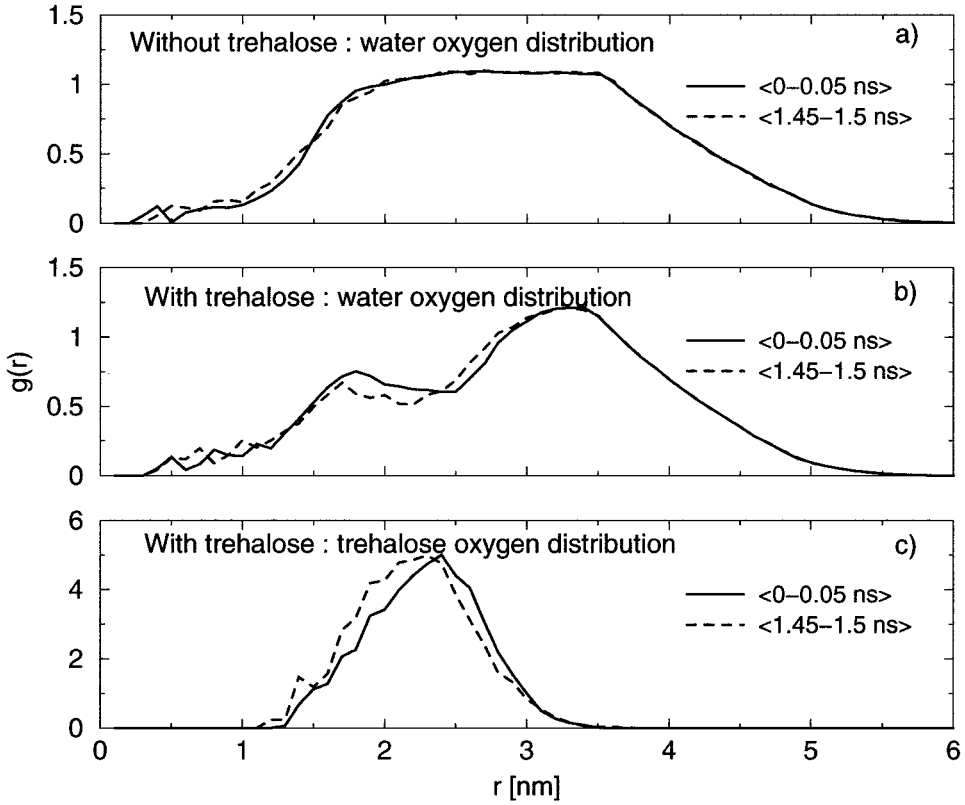

Fig. 5. Radial distribution functions [$g(r)$] for water and trehalose oxygens around the center of geometry of the protein (**a**) in the absence or (**b,c**) in the presence of trehalose. Data is averaged over 0.5 ns intervals corresponding to initial and equilibrated configurations, and computed using a bin width of 0.1 nm.

crease [Fig. 6(a)]. Rather, a slight decrease is observed during the course of the simulation. On the other hand, as an indirect effect of trehalose coating, the number of protein–water hydrogen bonds decreases by roughly a factor of four during the initial 0.8 ns of the simulation [Fig. 6(b)], corresponding to the equilibration of the trehalose molecules (Fig. 4). This observation suggests that the trehalose molecules efficiently compete with the protein for forming hydrogen bonds with the water molecules trapped in the thin layer at the protein surface. This interpretation is supported by a hydrogen-bond analysis restricted to the subset of water molecules that are at least once hydrogen bonded to the protein over the entire simulation (Table I). This subset of water molecules loses hydrogen bonds to trehalose at a much lower rate (roughly half as fast) compared to bulk water molecules. At the onset of the simulation, this subset of molecules actually gains hydrogen bonds to trehalose (+14 at 0.5 ns, but −11 at 1.0 ns, to finally reach −66 at 2.4 ns). However, in addition to this small increase in the number of trehalose–water hydrogen bonds close to the protein surface, the clustering of trehalose molecules provokes a very large loss of trehalose–water hydrogen bonds throughout the entire system, which dominates the overall time evolution of this quantity [Fig. 6(c)]. Finally, the number of trehalose–trehalose hydrogen bonds increases, while the number of protein–protein hydrogen bonds remains essentially unaffected (Table I). These observations are summarized in Figure 7 in the form of a proposed model for protein–trehalose interaction in aqueous (0.5 *M*) solution on the nanosecond timescale.

Protein Fluctuations

The root-mean-square atomic positional fluctuations (RMSF) calculated over the interval 1.0–1.5 ns for either C_α atoms only or averaged over all atoms of each residue is displayed as a function of the residue number in Figure 8. The calculated fluctuations for the C_α backbone atoms [Fig. 8(a)] show no significant difference regardless of the presence or absence of trehalose, the corresponding averages being 0.101 nm and 0.099 nm, respectively. However, a slight decrease in the side-chain fluctuations leads to reduced residue-averaged values for the system in the presence of trehalose [Fig. 8(b)], the corresponding averages being 0.155 nm and 0.166 nm, respectively. This result contrasts with previous observations of trehalose–protein interaction based on a simulation of myoglobin.[48] In this study, the addition of trehalose to the solvated protein was reported to considerably hinder the motion of all the apoprotein atoms at 300 K, including backbone atoms.[48] This discrepancy may arise from statistical inaccuracies due to the smaller length of the sampled trajectories (300 ps) or, more likely, from the significantly larger

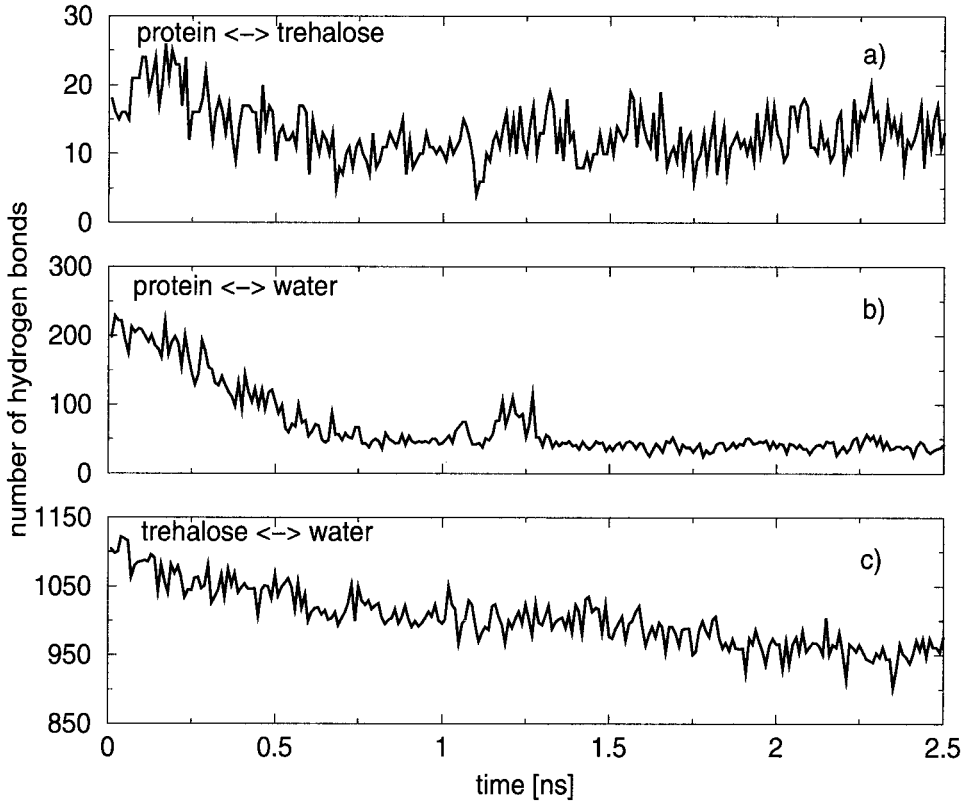

Fig. 6. Number of hydrogen bonds between (**a**) the protein and trehalose molecules, (**b**) the protein and water molecules, and (**c**) trehalose and water molecules during the simulation including trehalose. A hydrogen bond D–H · · · A is assumed to be present when the distance H · · · A is smaller than 0.25 nm and the angle D–H · · · A is larger than 135°.

TABLE I. Initial Value and Variation (Between Parentheses) of the Number of Hydrogen Bonds During the Simulation in the Presence of Trehalose, Defined by Averaging Over the Intervals 0.0–0.2 ns (Initial) Versus 2.3–2.5 ns (Final)

	Protein	Trehalose	Water	Water*
Protein	100 (0.0)	20 (−7)	199 (−161)	199 (−161)
Trehalose	—	353 (+22)	1085 (−133)	378 (−66)
Water	—	—	15492 (+82)	4460 (+129)
Water*	—	—	—	—

*Indicates an average restricted to the subset of water molecules once hydrogen bonded to the protein over the entire simulation.

trehalose concentration used in this other study (about 23 *M*).

CONCLUSIONS

The main alternative mechanisms of protein stabilization by trehalose proposed to rationalize the (partly contradictory) experimental data are: (1) the direct interaction between trehalose molecules and the protected biostructure through hydrogen bonds (water-replacement hypothesis)[23–26]; (2) the trapping of water molecules close to the biomolecular surface (water-layer hypothesis)[27]; (3) the entrapment of a particular biomolecular conformation in a high-viscosity trehalose matrix (mechanical-entrapment hypothesis).[28,29] It should be stressed that only the third mechanism represents a full explanation of trehalose stabilization, while the first two mechanisms are only descriptive (and, thus, not necessarily incompatible with the third mechanism). When interpreting the results of these simulations in terms of the three above-mentioned mechanisms, it should be kept in mind that these simulations only probe a given concentration range (moderately concentrated 0.5 *M* aqueous solution), a rather short timescale (2.5 ns), and systems at room temperature.

Keeping these restrictions in mind, the simulation results do not provide support for the water-replacement hypothesis. Although trehalose clusters around the protein, it does not expel the water molecules closest to the protein surface. Moreover, the number of protein–trehalose hydrogen bonds does not increase over the course of the simulation. This does not exclude, however, the fact that water-replacement may indeed occur over a longer timescale. In fact, it may be expected that the initial clustering of the trehalose molecules, leading to an increase of the local viscosity, would significantly slow down the occurrence of such a process. Experimentally, the mimicry of water molecules by sugar hydroxyl groups has been extensively investigated.[46,49–52] However, cocrystallization of lysozyme with trehalose, sorbitol, or sucrose did not affect significantly the protein hydration shell,[46] which

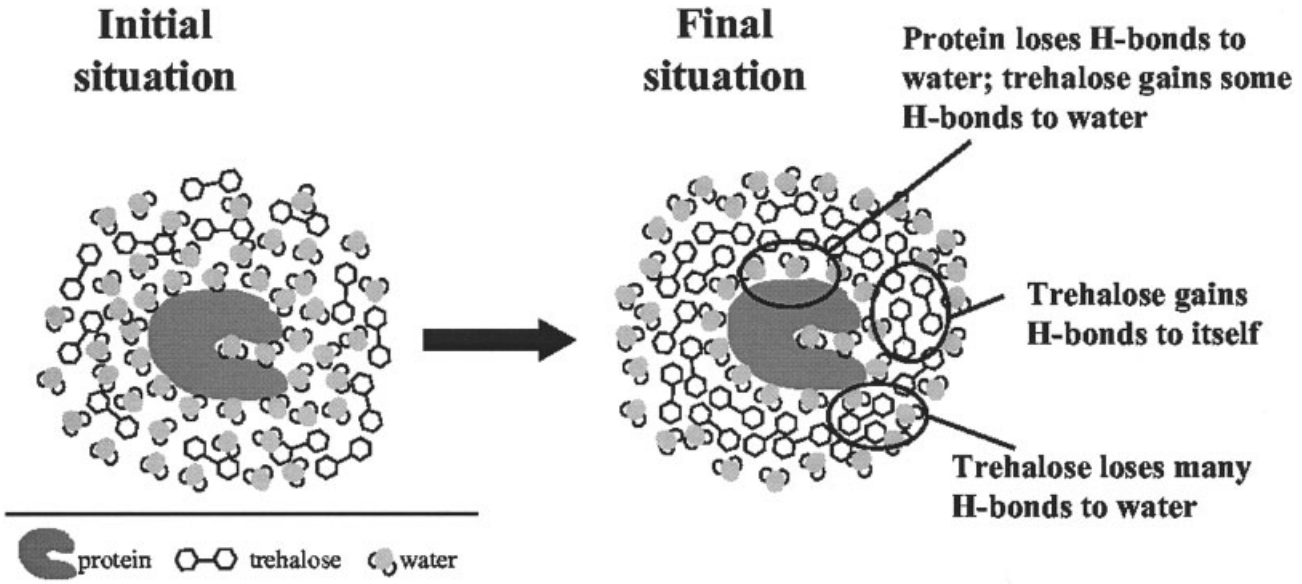

Fig. 7. Model for trehalose–protein interaction in aqueous solution on the nanosecond timescale. In the initial situation, trehalose is distributed homogeneously in solution. The presence of the protein induces a clustering of trehalose molecules and the trapping of a thin water layer at the protein surface. The trehalose molecules in the coating layer efficiently compete with the protein for forming hydrogen bonds with the water molecules in the trapped layer, effectively desolvating the protein. The overall process results in a loss of protein–water hydrogen bonds, a gain of trehalose–trehalose hydrogen bonds, and an overall loss of trehalose–water hydrogen bonds (because the gain of such hydrogen bonds at the protein surface is overcompensated by a corresponding loss in the bulk, due to trehalose clustering).

hints toward the absence of a strong direct interaction between the protein and these additives, and suggests that the stabilizing effect of carbohydrates should be sought outside the immediate neighborhood of the protein.[46]

Neither do the simulation results provide support for the mechanical-entrapment hypothesis. Although the clustering of trehalose close to the protein surface leads to slightly reduced deviations of the side-chain conformations from the crystal structure, and to slightly reduced side-chain conformational fluctuations, no such effect is observed for the backbone of the protein. These observations are in agreement with the suggestion that trehalose does not affect significantly the dynamics of biostructures under ideal conditions (i.e., in solution at room temperature).[2,46,47] However, this conclusion is restricted to the moderate concentration range probed in the present study. There is little doubt that trehalose coating significantly reduces the protein flexibility in more concentrated solutions or in dry (glassy) trehalose matrices, based on both experimental[53] and theoretical[48] evidence.

Finally, these present simulation results are most easily interpreted in the context of the water-layer hypothesis,[27] because it appears that such a layer is indeed preserved at the protein surface on the nanosecond timescale. This is in good agreement with the experimental observation that, unlike other sugars, trehalose in aqueous solution is totally excluded from the first hydration shell of a protein.[54] This may be due to the fact that the hydrated volume of trehalose is anomalously high (i.e., at least 2.5-fold larger compared to other common sugars, such as sucrose, maltose, glucose, and fructose.[55] Furthermore, the simulation suggests that this trapped water layer may possess peculiar properties. Because the trehalose molecules efficiently compete with the protein for the formation of hydrogen bonds with the trapped water molecules (Fig. 7), thereby reducing the number of protein–solvent hydrogen bonds by a factor of four, this water layer is expected to show reduced electrostatic solvation properties toward the protein. Such a reduction of the solvation might be responsible for a compensating enhancement of intraprotein interactions and, thus, a stabilization of the protein native structure. The existence of such a thin water layer trapped between a matrix of additive and the protein surface, and characterized by limited solvation properties, may help to explain some experimental observations. For example, *Desulfovibrio gigas* rubredoxin in a solution of 1,1-diglycerol phosphate (0.1 *M*) is characterized by significantly decreased amide proton exchange rates in the region of the protein interacting with the additive.[56] Such slow exchange rates suggest a weakened interaction of these protons with the solvent and, possibly, increased stability of the protein.[57,58]

The goal of this study was to use MD simulations to shed some light on the mechanism of protein stabilization by trehalose. Analysis of the simulation results led to the suggestion of a model at the molecular level for protein–trehalose interactions in moderately concentrated aqueous solutions, at room temperature, and on the nanosecond timescale. Clearly, additional MD simulations will be required, involving different biomaterials, and under a wider range of conditions of concentration and temperature (some of which are under way), to provide a more complete understanding of the overall mechanism for the trehalose-induced stabilization of biostructures.

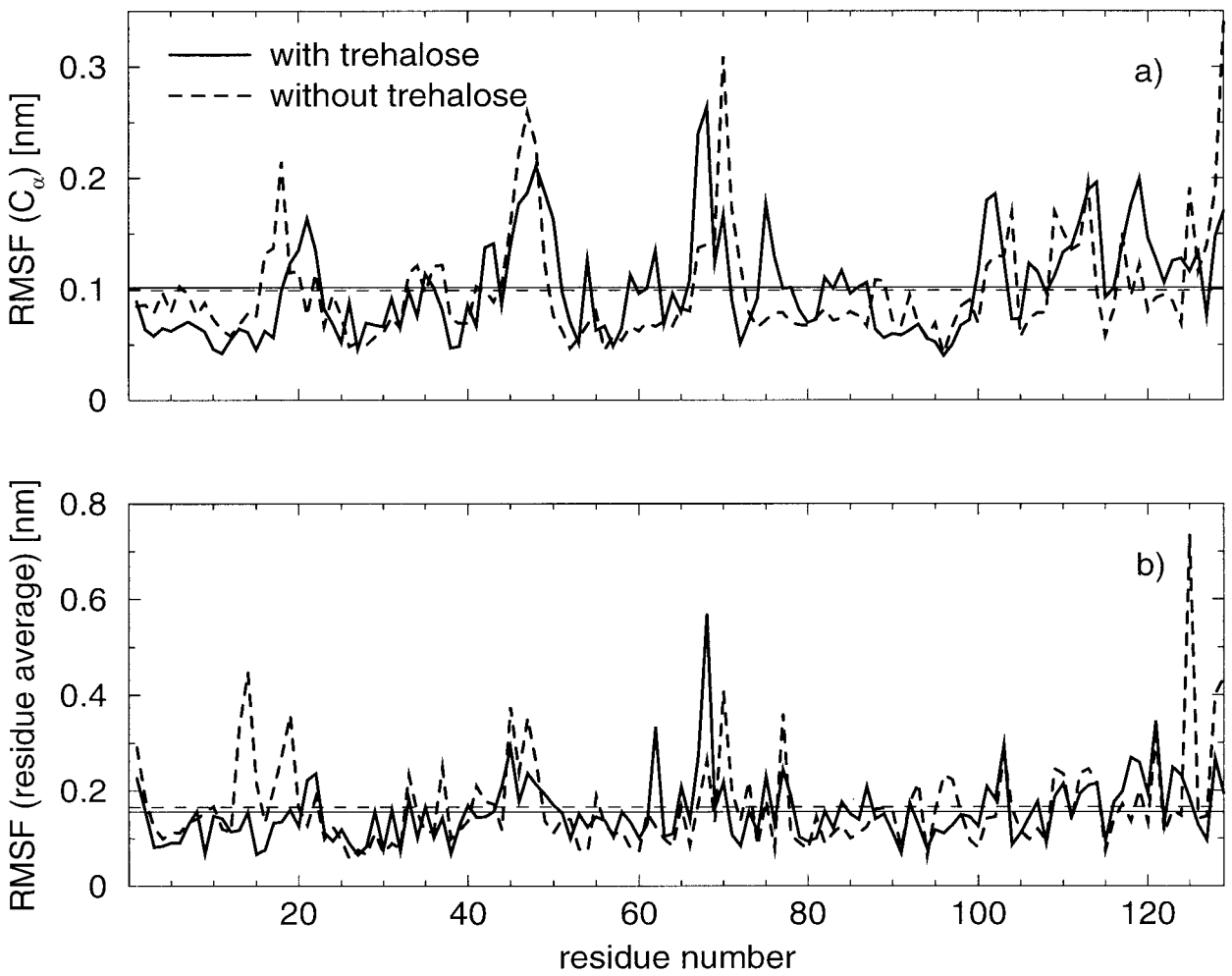

Fig. 8. Root-mean-square atomic positional fluctuations (RMSF) (**a**) for C_α carbon atoms and (**b**) averaged over all atoms of a residue, averaged over the 1.0–1.5 ns interval for the systems in presence (solid line) or in absence (dashed line) of trehalose. The thin horizontal lines represent the corresponding average values for all residues.

ACKNOWLEDGMENTS

We would like to thank Professor John F. Carpenter for valuable discussions during the setup of this simulation. Professor Claudio Soares is acknowledged for insightful comments on the stabilization of proteins by compatible solutes. The NWChem 4.1 computational chemistry package for massive parallel computers used in this study was developed by the High Performance Computational Chemistry group, Environmental Molecular Sciences Laboratory, Pacific Northwest National Laboratory. Battelle Memorial Institute operates Pacific Northwest National Laboratory for the U.S. Department of Energy.

REFERENCES

1. Crowe JH, Crowe LM, Carpenter JF, Wistrom CA. Stabilization of dry phospholipid bilayers and proteins by sugars. Biochem J 1987;242:1–10.
2. Crowe JH, Crowe LM, Oliver AE, Tsvetkova N, Wolkers W, Talbin F. The trehalose myth revisited: Introduction to a symposium on stabilization of cells in the dry state. Cryobiology 2001;43:89–105.
3. Richards AB, Krakowka S, Schmid LBDH, Wolterbeek APM, Waalkens-Berendsen DH, Shigoyuki A, Kurimoto M. Trehalose: a review of properties, history of use and human tolerance. Food Chem Toxicol 2002;40:871–898.
4. Chen T, Fowler A, Toner M. Literature review: supplemented phase diagram of the trehalose–water binary mixture. Cryobiology 2000;40:277–282.
5. Elbein AD. The metabolism of α,α-trehalose. In: Tipson RS, Horton D., Editors. Advances in carbohydrate chemistry and biochemistry. Vol. 30. Academic Press: New York, 1974 pp. 227–256.
6. Wyatt GR, Kalf GF. The chemistry of insect hemolymph: II. Trehalose and other carbohydrates. J Gen Physiol 1957;40:833–847.
7. Adams RP, Kendall E,, Kartha KK. Comparison of free sugars in growing desiccated plants of *Selaginella lepidophylla*. Biochem Syst Ecol 1990;18:107–110.
8. Westh P, Ramlov H. Trehalose accumulation in the tardigrade *Adorybiotus coronifer* during anhydrobiosis. J Exp Zool 1991;258:303–311.
9. Clegg JS. Origin of trehalose and its significance during formation of encysted dormant embryos of *Artemia salina*. Comp Biochem Physiol 1965;14:135–143.
10. Huggins AK, Boulton AP. Metabolism of trehalose during morphogenesis of brine shrimp *Artemia salina*. Biochem J 1970;117:42–43.
11. Clegg JS. Cryptobiosis—a peculiar state of biological organization. Comp Biochem Phys B 2001;128:613–624.
12. Feofilova EP. Deceleration of vital activity as a universal biochemical mechanism ensuring adaptation of microorganisms to stress factors: a review. Appl Biochem Micro 2003;39:1–18.

13. Nakagaki M, Nagasse H, Ueda H. Stabilization of the lamellar structure of phosphatidylcholine by complex formation with trehalose. J Mol Sci 1992;73:173–180.
14. Hoekstra FA, Wolkers WF, Buitink J, Golovina EA, Crowe JH, M. Crowe L. Membrane stabilization in the dry state. Comp Biochem Phys A 1997;117:335–341.
15. Takahashi H, Ohmae H, Hatta I. Trehalose-induced destabilization of interdigitated gel phase in dihaxadecylphosphatidylcholine. Biophys J 1997;73:3030–3038.
16. Carpenter JF, Crowe JH. Modes of stabilization of a protein by organic solutes during desiccation. Cryobiology 1988;25:459–470.
17. Xie GF, Timasheff SN. The thermodynamic mechanism of protein stabilization by trehalose. Biophys Chem 1997;64:25–43.
18. Robinson CH. Cold adaptation in arctic and antarctic fungi. New Phytol 2001;151:341–353.
19. Wang GM, Haymet ADJ. Trehalose and other sugar solutions at low temperature: Modulated differential scanning calorimetry. J Phys Chem B 1998;102:5341–5347.
20. Crowe JH, Carpenter JF, Crowe LM, Anchordoguy T. Are freezing and dehydration similar stress vectors?: A comparison of modes of interaction of stabilizing solutes with biomolecules. Cryobiology 1990;27:219–231.
21. Carninci P, Nishiyama Y, Westover A, Itoh M, Nagoaka S, Ki NS, Okazaki Y, Muramatsu M, Hayashizaki Y. Thermostabilization and thermoactivation of thermolabile enzymes by trehalose and its application for the synthesis of full length cDNA. Proc Natl Acad Sci USA 1998;95:520–524.
22. http://www.lineatrehalose.it.
23. Prestrelski S, Tedeschi N, Arakawa T, Carpenter JF. Dehydration-induced conformational transitions in proteins and their inhibition by stabilizers. Biophys J 1993;65:661–671.
24. Carpenter JF, Crowe JH. An infrared spectroscopic study of the interactions of carbohydrates with dried proteins. Biochemistry 1989;28:3916–3922.
25. Crowe JH, Carpenter JF, Crowe LM. The role of vitrification in anhydrobiosis. Annu Rev Physiol 1998;6:73–103.
26. Allison SD, Chang B, Randolph TW, Carpenter JF. Hydrogen bonding between sugar and protein is responsible for inhibition of dehydration-induced protein unfolding. Arch Biochem Biophys 1999;365:289–298.
27. Belton PS, Gil AM. IR and raman-spectroscopic studies of the interaction of trehalose with hen egg-white lysozyme. Biopolymers 1994;34:957–961.
28. Ansari A, Jones CM, Henry ER, Hofrichter J, Eaton WA. The role of solvent viscosity in the dynamics of protein conformational-changes. Science 1992;256:1796–1798.
29. Hagen SJ, Hofrichter J, Eaton WA. Protein reaction-kinetics in a room-temperature glass. Science 1995;269:959–962.
30. Vaney MC, Maignan S, RiesKautt M, Ducruix A. High-resolution structure (1.33 Å) of a hen lysozyme tetragonal crystal grown in the apcf apparatus: data and structural comparison with a crystal grown under microgravity from Spacehab-01 mission. Acta Crystallogr D Biol Crystallogr 1996;52:505–517.
31. Berendsen HJC, Grigera JR, Straatsma TP. The missing term in effective pair potential. J Phys Chem 1987;91:6269–6271.
32. Cornell WD, Cieplak P, Bayly CI, Gould IR, Merz KM, Ferguson DM, Spellmeyer DC, Fox T, Caldwell JW, Kollman PA. A 2nd generation force-field for the simulation of proteins, nucleic-acids and organic-molecules. J Am Chem Soc 1995;117:5179–5197.
33. Woods RJ, Chapelle R. Restrained electrostatic potential atomic partial charges for condensed-phase simulations of carbohydrates. J Mol Struct Theochem 1998;527:149–156.
34. Harrison RJ, Nichols JA, Straatsma TP, Dupuis M, Bylaska EJ, Fann GI, Windus TL, Apra E, Anchell J, Bernholdt D, Borowski P, Clark T, Clerc D, Dachsel H, de Jong B, Deegan M, Dyall K, Elwood D, Fruchtl H, Glendenning E, Gutowski M, Hess A, Jaffe J, Johnson B, Ju J, Kendall R, Kobayashi R, Kutteh R, Lin Z, Littlefield R, Long X, Meng B, Nieplocha J, Niu S, Rosing M, Sandrone G, Stave M, Taylor H, Thomas G, van Lenthe J, Wolinski K, Wong A, Zhang Z. NWChem, a computational chemistry package for parallel computers, version 4.0 Richland, WA: Pacific Northwest National Laboratory; 2000.
35. Berendsen HJC, Postma JPM, van Gunsteren WF, DiNola A, Haak JR. Molecular dynamics coupling to an external bath. J Chem Phys 1984;81:3684–3690.
36. Esmann U, Perera L, Berkowitz ML, Darden T, Lee H, Pedersen LG. A smooth particle mesh Ewald method. J Chem Phys 1995;103: 8577–8593.
37. Ryckaert JF, Ciccotti G, Berendsen HJC. Numerical-integration of Cartesian equations of motion of a system with constraints—molecular-dynamics of *n*-alkanes. J Comp Phys 1977;23:327–341.
38. Hockney RW. The potential calculation and some applications. Methods Comput Phys 1970;9:136–211.
39. Damm W, Frontera A, Tirado-Rives J, Jorgensen WL. OPLS all-atom force field for carbohydrates. J Comput Chem 1997;18: 1955–1970.
40. Kony D, Damm W, Stoll S, van Gunsteren WF. An improved OPLS-AA force field for carbohydrates. J Comput Chem 2002;23: 1416–1429.
41. Woods RJ, Dwek RA, Edge CJ. Molecular mechanical and molecular dynamical simulations of glycoproteins and oligosaccharides: 1. GLYCAM 93 parameter development. J Phys Chem 1995;99: 3832–3846.
42. Bayly CI, Cieplak P, Cornell WD, Kollman PA. A well-behaved electrostatic potential based method using charge restraints for deriving atomic charges—the RESP model. J Phys Chem 1993;97: 10269–10280.
43. Batta G, Kövér KE, Gervay Hornyák M, Roberts GM. Temperature dependence of molecular conformation, dynamics and chemical shift anisotropy of α, α-trehalose in D2O by NMR relaxation. J Am Chem Soc 1997;119:1336–1345.
44. Duda CA, Stevens ES. Trehalose conformation in aqueous-solution from optical-rotation. J Amer Chem Soc 1990;112:7406–7407.
45. Kabsh W, Sander C. Dictionary of protein secondary structure: Pattern recognition of hydrogen-bonded and geometrical features. Biopolymers 1983;22:2577–2637.
46. Datta S, Biswal BK, Vijayan M. The effect of stabilizing additives on the structure and hydration of proteins: a study involving tetragonal lysozyme. Acta Crystallogr D Biol Crystallogr 2001;57: 1614–1620.
47. Saraswathi NT, Sankaranarayanan R, Vijayan M. Effect of stabilizing additives on the structure and hydration of proteins: a study involving monoclinic lysozyme. Acta Crystallogr D Biol Crystallogr 2002;58:1162–1167.
48. Cottone G, Cordone L, Ciccotti G. Molecular dynamics simulation of carboxy-myoglobin embedded in a trehalose–water matrix. Biophys J 2001;8:931–938.
49. Delbaere LTJ, Vandonselaar M, Prasad L, Quail JW, Wilson KS, Dauter Z. Structures of the lectin-iv of *Griffonia simplicifolia* and its complex with the Lewis-b human blood-group determinant at 2.0 Å resolution. J Mol Biol 1993;230:950–965.
50. Delbaere LTJ, Vandonselaar M, Quail LPJW, Pearlstone JW, Carpenter MR, Smillie LB, Nikrad PV, Spohr U, Lemieux LU. Molecular recognition of a human blood-group determinant by a plant lectin. Can J Chem 1990;68:1116–1121.
51. Elgavish S, Shaanan B. Structures of the *Erythrina corallodendron* lectin and of its complexes with mono- and disaccharides. J Mol Biol 1998;277:917–932.
52. Ravishankar R, Suguna K, Surolia A, Vijayan M. Structures of the complexes of peanut lectin with methyl-beta-galactose and *n*-acetyllactosamine and a comparative study of carbohydrate binding in Gal/GalNAc-specific legume lectins. Acta Crystallogr D Biol Crystallogr 1999;55:1375–1382.
53. Tsai AM, Neumann DA, Bell LN. Molecular dynamics of solid-state lysozyme as affected by glycerol and water: a neutron scattering study. Biophys J 2000;79:2728–2732.
54. Lin TY, Timasheff SN. On the role of surface tension in the stabilization of globular proteins. Prot Sci 1996;5:372–381.
55. Sola-Penna M, Meyer-Fernandes JR. Stabilization against thermal inactivation promoted by sugars on enzyme structure and function: why is trehalose more effective than other sugars? Arch Biochem Biophys 1996;360:10–14.
56. Lamosa P, Brennan L, Vis H, Turner DL, Santos H. NMR structure of *Desulfovibrio gigas* rubredoxin: a model for studying protein stabilization by compatible solutes. Extremophiles 2001;5: 303–311.
57. Wagner G, Wütrich K. Correlation between the amide proton exchange rates and the denaturation temperatures in globular protein related to the basic pancreatic trypsin inhibitor. J Mol Biol 1979;130:31–37.
58. Englander SW, Sosnick TR, Englander JJ, Mayne L. Mechanisms and uses of hydrogen exchange. Curr Opin Struct Biol 1996;6:18–23.